



Low-Temperature Oxidation of Particulate Matter Using Ozone

Journal:	<i>RSC Advances</i>
Manuscript ID:	RA-ART-02-2014-001003.R1
Article Type:	Paper
Date Submitted by the Author:	11-Apr-2014
Complete List of Authors:	Itoh, Yoshihiko; Toyota Central R&D Labs., Inc., Sakabibara, Yuji; Toyota Central R&D Labs., Inc., Shinjoh, Hirofumi; Toyota Central R&D Labs., Inc.,

1 Low-Temperature Oxidation of Particulate Matter

2 Using Ozone

3 *Yoshihiko Itoh**, *Yuji Sakakibara* and *Hirofumi Shinjoh*

4 TOYOTA CENTRAL R&D LABS., INC.

5 41-1 Yokomichi, Nagakute, Aichi 480-1192, Japan

6 Low-temperature oxidation of particulate matter (PM) was investigated using ozone, which has
7 high oxidation ability. Granular carbon was first used as a model PM to investigate the influential
8 factors for PM oxidation with ozone. The PM collected from diesel exhaust using a diesel
9 particulate filter was then evaluated to determine the oxidation performance of ozone. Carbon
10 was effectively oxidized by ozone at low temperatures less than 573 K and the oxidation rate was
11 larger than ten times that for NO₂ at 423 K; however, the oxidation rates were decreased by the
12 thermal decomposition of ozone and reaction with NO as an exhaust gas component. The
13 oxidation rate when using ozone could be calculated with inclusion of these factors using the
14 Arrhenius equation. The PM oxidation characteristics were similar to those for granular carbon.
15 The results indicate that oxidation with ozone is a promising method for low-temperature PM
16 oxidation and optimized performance with ozone could be achieved.

17 1. INTRODUCTION

18 Diesel particulate filters (DPFs) used for the reduction of particulate matter (PM) emissions from
19 diesel engines require appropriate regeneration by the oxidation of PM accumulated in the DPF
20 because accumulated PM causes clogging of the DPF, which decreases engine performance and
21 efficiency by increasing exhaust backpressure. Although PM oxidation using high-temperature
22 exhaust gas by the addition of extra fuel into the exhaust system is generally used for DPF
23 regeneration, it is difficult to execute this method for low exhaust temperature, such as the
24 conditions experienced under traffic congestion.

25 NO_2 generated from NO contained in diesel exhaust gas has been applied for the regeneration
26 of DPFs used with commercial diesel engines.¹ However, high NO_2 concentrations are required
27 to achieve sufficient PM oxidation rates at low temperatures. Moreover, the NO oxidation
28 performance of the oxidation catalyst is decreased at low temperatures, which leads to an
29 increase of NO_x emissions.

30 Non-thermal plasma (NTP) has been proposed as a solution to this problem.^{2,3} This method has
31 potential for low-temperature PM oxidation with reasonable energy consumption to generate
32 NTP, but it has not yet been applied practically, due to difficulties in the attachment of the
33 reactor setup to conventional exhaust systems, such as DPFs, and lack of reliability for high-
34 voltage electrode operation in the exhaust gas.

35 Ozone has higher activity as an oxidant than Cl_2 or H_2O_2 , and harmful effects to the
36 environment and human health are eliminated by the thermal decomposition of ozone to O_2 .
37 Ozone has low reactivity with carbon or PM under atmospheric conditions;⁴ however, it has been
38 reported that PM oxidation is promoted by ozone⁵ and that ozone injection to diesel exhaust is
39 effective for direct PM oxidation by ozone or by NO_2 generated through the ozone-NO reaction.⁶
40 There have been various PM oxidation rates reported from different investigations and the
41 essential PM oxidation properties of ozone under the conditions of diesel exhaust remain unclear

42 because the quantitative effects of temperature and the exhaust gas components have yet to be
43 clarified.^{5,6} Therefore, we have investigated the applicability of low-temperature PM oxidation
44 using ozone with particular focus on the effect of temperature and the presence of other
45 components contained in diesel exhaust gas.

46

47 2. EXPERIMENTAL

48 The experimental setup used in this study is presented in Fig. 1. The PM oxidation properties of
49 ozone were investigated according to the following steps. Firstly, to investigate the fundamental
50 oxidation properties of ozone, granular carbon (Kishida Chemical Co. Ltd., 1-1.7 mm pellets,
51 reagent grade, 3 mL) was used as a model PM with crushed quartz (1-1.7 mm pellets, 7 mL).
52 Secondly, PM collected from the DPF (30 mm diameter, length 50 mm, 0.155 cells/cm²) of an
53 automotive diesel engine (2 L displacement, 4-cylinder, direct injection) was evaluated. The
54 engine operation conditions were a torque of 30 Nm at 2000 rpm and the amount of PM collected
55 was 80 mg. After the PM was collected, the DPF was heat treated at 573 K for 1 h in air to
56 remove the soluble organic fraction (SOF). A straight flow system was applied by modification
57 of the DPF, as shown by the PM in the DPF section of Fig. 1, to eliminate the effect of the
58 accumulated PM on the filter surfaces for constant PM oxidation.

59 A gas generator was used to mix N₂, H₂O, NO, NO₂, C₃H₆ and CO as the model diesel exhaust
60 gas, in addition to an ozonizer (Nippon Ozone Co. Ltd., IO-1A6). The oxidation rate was
61 measured according to the CO and CO₂ concentrations, which were measured using a non-
62 dispersive infrared analyzer (Shimadzu Corp., GCT-7000). Ozone and other gas components
63 were measured using an ozone monitor (Ebara Jitsugyo, Co. Ltd., PG-620 PA) and an exhaust
64 gas analyzer (Horiba, Ltd., MEXA-9100D), respectively. The experimental conditions employed

65 are shown in Tables 1 and 2 for PM carbon oxidation (PM and C ox.), the thermal decomposition
66 of ozone (O₃ decomp.) and the reaction of ozone with other gas components (O₃ react.).

67 The accuracy for the ozone concentration measurements was 1%, and that for other gas
68 components was within 2%. The temperature of the reaction vessel for the oxidation of carbon or
69 PM in DPFs was controlled to within 1 K.

70

71 3. RESULTS AND DISCUSSION

72 3.1 FUNDAMENTAL STUDY ON THE OXIDATION OF CARBON USING OZONE

73 The temperature dependence of the carbon oxidation rate using ozone is shown in Fig. 2. Carbon
74 was oxidized by ozone at low-temperature conditions under 573 K. The carbon oxidation rate
75 increased with the amount of supplied ozone (inlet ozone concentration) and had a maximum at
76 523 K. For quantitative evaluation, the oxidation rates calculated using the Arrhenius equation
77 represented in Eq. 1 are also shown in Fig. 2.

78

$$79 \quad r = 79.883 C_{\text{O}_3, \text{supp.}} e^{-2088.5/T}, \quad (1)$$

80

81 where r is the rate of carbon oxidation (mmol/h), $C_{\text{O}_3, \text{supp.}}$ is the amount of supplied ozone
82 (mmol/h), and T is the temperature (K).

83 However, the oxidation rates calculated using Eq. 1 correspond well with the experimental
84 values for supplied ozone from 5 to 25 mmol/h (190 to 930 ppm) at temperatures below 423 K.
85 The difference between the calculated and experimental oxidation rates increased with the
86 temperature at over 423 K. The calculated oxidation rates increased monotonically with the
87 temperature, whereas the experimental values decreased at 573 K.

88 The thermal decomposition of ozone occurs increasingly at higher temperature. The deviation
 89 between the calculated and experimental oxidation rates may be attributed to a decrease in the
 90 amount of ozone reacting with carbon due to thermal decomposition. Thus, the thermal
 91 decomposition properties of ozone were measured by removing carbon from the apparatus and
 92 described using another Arrhenius equation:

93

$$94 \quad C_{O_3, T} = 1000 C_{O_3, \text{supp.}}^{1.22} e^{-4440/T}, \quad (2)$$

95

96 where $C_{O_3, T}$ is the amount of thermally decomposed ozone (mmol/h).

97 Figure 3 shows that the ozone residual ratio decreases over 400 K, which indicates significant
 98 decomposition of ozone at higher temperatures and almost complete decomposition at over 573
 99 K. Figure 4 shows the experimental and calculated (Eq. 2) temperature dependence of the ozone
 100 thermal decomposition rate. The experimental results correspond well with that calculated from
 101 Eq. 2.

102 Figure 5 shows the temperature dependence of the carbon oxidation rate calculated using Eq.
 103 3, which combines Eqs. 1 and 2, compared with the experimental carbon oxidation rates.
 104 Equation 3 describes the decrease in the oxidation rate of carbon at higher temperatures with
 105 good correspondence to the experimental results for temperatures up to 573 K. Therefore, the
 106 temperature dependence of the carbon oxidation rate using ozone could be successfully
 107 calculated with consideration of the thermal decomposition of ozone.

108

$$109 \quad r_T = 79.883 (C_{O_3, \text{supp.}} - C_{O_3, T}) e^{-2088.5/T}, \quad (3)$$

110

111 where r_T is the rate of carbon oxidation with the thermal decomposition of ozone (mmol/h).

112 It appears that the carbon oxidation rate with ozone is dependent on the residual amount of
113 ozone at the carbon. These results indicate that those gas components that have high reactivity
114 with ozone would decrease the carbon oxidation rate. The rate constants for the reaction of
115 various gas components with ozone were reported to be in the following order: $\text{NO} > \text{NO}_2 >$
116 $\text{C}_3\text{H}_6 > \text{SO}_2 > \text{C}_3\text{H}_8 > \text{CH}_4 > \text{CO}$.⁷⁻¹² Figure 6 shows the residual ratio of ozone reacted with NO,
117 NO_2 , C_3H_6 and CO; the results indicate that ozone is entirely consumed by NO with the lowest
118 concentration, whereas CO has no effect on the ozone residual ratio. The order of reactivity with
119 ozone was $\text{NO} > \text{NO}_2 > \text{C}_3\text{H}_6 > \text{CO}$, which is consistent with previously reported results.⁷⁻¹²

120 Therefore, NO would significantly decrease the carbon oxidation rate by ozone consumption.
121 The amount of the ozone consumption can be estimated by evaluating the ozone/NO reaction
122 ratio both experimentally and by calculation using Eq. 4, and the results are shown in Fig. 7. The
123 reaction ratio was larger than 1 and increased with temperature, which may be due to the
124 formation of NO_3 and N_2O_5 in addition to NO_2 .¹³ The amount of ozone reaction with NO can be
125 described by Eq. 5 using Eq. 4:

126

$$127 \quad k_{\text{O}_3, \text{NO}} = 0.65316 e^{0.00286T}, \quad (4)$$

$$128 \quad C_{\text{O}_3, \text{NO}} = k_{\text{O}_3, \text{NO}} C_{\text{NO}}, \quad (5)$$

129

130 where $k_{\text{O}_3, \text{NO}}$ is the ozone/NO reaction ratio, $C_{\text{O}_3, \text{NO}}$ is the amount of ozone reacted with NO
131 (mmol/h), and C_{NO} is the amount of inlet NO (mmol/h).

132 Considering these results, the ozone-NO reaction would be faster than the thermal
133 decomposition of ozone. Therefore, ozone at the inlet would be consumed by the ozone-NO
134 reaction before thermal decomposition could occur. The amount of thermally decomposed ozone
135 with NO could thus be explained by Eq. 6. Consequently, the carbon oxidation rate with NO

136 could be explained by Eq. 7 from a combination of Eqs. 1 to 6. Figure 8 shows the calculated
 137 results for the carbon oxidation rate using ozone containing NO from Eq. 7, in addition to the
 138 experimental results. The calculated results correspond well with the experimental results for
 139 ozone supplied at 15 to 25 mmol/h (560 to 930 ppm) at 423 K. Consequently, the oxidation rate
 140 of carbon using ozone with consideration of the effect of NO reaction and thermal decomposition
 141 is well described by Eq. 7:

142

$$143 \quad C_{O_3, T, NO} = 1000 (C_{O_3, \text{supp.}} - C_{O_3, NO})^{1.22} e^{-4440/T}, \quad (6)$$

$$144 \quad r_{T, NO} = 79.883 (C_{O_3, \text{supp.}} - C_{O_3, NO} - C_{O_3, T, NO}) e^{-2088.5/T}, \quad (7)$$

145

146 where $C_{O_3, T, NO}$ is the amount of thermally decomposed ozone and that reacted with NO
 147 (mmol/h), and $r_{T, NO}$ is the oxidation rate with thermal decomposition and reaction of ozone with
 148 NO (mmol/h).

149 To simulate the exhaust gas, ion exchanged water was added to the inlet N_2 gas; however,
 150 water vapor contained in the exhaust gas had no effect on the rate of carbon oxidation using
 151 ozone.

152

153 3.2 APPLICATION OF OZONE FOR PM OXIDATION

154 PM oxidation was conducted using ozone and compared with the results for carbon oxidation,
 155 and the results are shown in Fig. 9. The PM oxidation rate using ozone was similar to that for
 156 carbon at 373 and 423 K, which confirms that the carbon material used in this study was suitable
 157 as a model material for PM oxidation.

158 The PM oxidation rates with various gas components at 423 K are shown in Fig. 10. The PM
 159 oxidation rate with ozone decreased significantly in the presence of NO. For gas containing

160 ozone and NO₂, the effect on the PM oxidation rate was less than that for ozone and NO. Without
161 ozone, NO and NO₂ showed extremely low efficiency for PM oxidation at 423 K. Thus, PM
162 oxidation by NO₂¹ is ineffective under low-temperature conditions. At the same temperature,
163 NO is completely oxidized to NO₂ by reaction with ozone and the supplied ozone is entirely
164 consumed, so that the PM oxidation rate using ozone containing NO was similar to that for NO₂
165 without ozone.

166 From these results, the optimum amount of supplied ozone for effective PM oxidation could be
167 elucidated. Although these results show that ozone is effective for the oxidation of PM,
168 countermeasures to inhibit ozone consumption by the ozone-NO reaction are required for the
169 effective utilization of ozone for PM oxidation. NO_x reduction, NO oxidation to NO₂ or an
170 intermittent supply of high-concentration ozone relative to NO would be effective for this
171 purpose.

172 In contrast, the PM oxidation rate using ozone was much higher than that reported previously
173 from thermogravimetric analysis (TGA).⁵ This would be presumed to enhance the thermal
174 decomposition of ozone and lower the contact probability of ozone and PM relative to this
175 experiment, due to the long residence time of ozone in the vessel and the small contact area of
176 PM on the TGA sample pan.

177 The specific ozone yields for an industrial ozone generator are reported to be around 100
178 g/kWh.^{14,15} The oxidation rate of PM at 473 K in this study was estimated to be 7–10 g/kWh
179 when including countermeasures for NO, which is similar to PM oxidation by NTP.²
180 Consequently, ozone is suitable for the regeneration of a DPF with consideration of the fuel
181 efficiency penalty (1%) with ozone generation.

182 High-temperature exhaust gas for high load during engine operation would cause a decrease in
183 the PM oxidation rate. This could be avoided by lowering the exhaust gas temperature by setting

184 the DPF near the tailpipe and/or by injecting cooling air into the exhaust in front of the DPF. The
185 harmful effects of residual ozone to the environment and on human health could be removed by
186 setting an ozone decomposition catalyst after the DPF. Although this method has some problems
187 in practical application, we consider that these could be addressed with such solutions.

188

189 4. CONCLUSIONS

190 A high oxidation rate of carbon used as a model PM was achieved using ozone at low
191 temperature below 523 K. However, the thermal decomposition of ozone at temperatures
192 exceeding 523 K and the reaction of ozone with NO decreased the oxidation rate. The carbon
193 oxidation rate could be described with inclusion of these effects using an Arrhenius equation, and
194 this could be applied for the oxidation of PM. These results indicate that the oxidation of PM
195 with ozone is a promising low-temperature PM oxidation method and that the optimum PM
196 oxidation performance applied for the actual exhaust systems of diesel engines could be
197 estimated.

198

199 ACKNOWLEDGMENT

200 The authors thank Dr. H. Hirata, M. Kakinohana and M. Ibe (Toyota Motor Co. Ltd.) for PM
201 sampling and discussion regarding the experiments.

202

203 REFERENCES

204 (1) S. Chatterjee, R. Conway and A. P. Walker, *SAE Technical Paper*, 2001, 2001-28-0049.

205 (2) S. Yao, E. Suzuki and A. Nakayama, *J. Hazard. Mater.*, 2001, **83(3)**, 237-242.

- 206 (3) K. Naito, Y. Kim, H. Fujikawa, T. Ogawa, I. Tan, K. Hasegawa, H. Tanaka, K. Madokoro,
207 S. Yao, Y. Fujioka and C. Fushimi, *JSAE Annual Congress Proceedings*, 2007, 20075740.
- 208 (4) T. A. Metts, S. A. Batterman, G. I. Fernandes and P. Kalliokoski, *Atmos. Environ.*, 2005,
209 **39(18)**, 3343-3354.
- 210 (5) S. Yao, C. Mine, C. Fushimi, K. Madokoro, S. Kodama, S. Yamamoto, Y. Fujioka, Y. Kim,
211 K. Naito, H. Fujikawa, T. Ogawa, I. Tan, K. Hasegawa and H. Tanaka, *JSAE Annual Congress*
212 *Proceedings*, 2007, 20075799.
- 213 (6) M. Okubo, N. Arita, T. Kuroki and T. Yamamoto, *JSAE Annual Congress Proceedings*,
214 **2005**, 20055437.
- 215 (7) H. H. Lippmann, B. Jesser and U. Schurath, *Int. J. Chem. Kinet.*, 1980, **12(8)**, 547-554.
- 216 (8) W. B. DeMore, S. P. Sander, D. M. Golden, R. F. Hampson, M. J. Kurylo, C. J. Howard, A.
217 R. Ravishankara, C. E. Kolb and M. J. Molina, *JPL Publication*, 1997, **97(4)**, 1-266.
- 218 (9) C. R. Greene and R. Atkinson, *Int. J. Chem. Kinet.*, 1992, **24(9)**, 803-811.
- 219 (10) R. J. Morrissey and C. C. Schubert, *Combust. Flame*, 1963, **7**, 263-268.
- 220 (11) F. J. Dilleuth, D. R. Skidmore and C. C. Schubert, *J. Phys. Chem.*, 1960, **64(10)**, 1496-
221 1499.
- 222 (12) M. A. Louis and P. Warneck, *J. Phys. Chem.*, 1972, **76(11)**, 1514-1516.
- 223 (13) R. A. Graham and H. S. Johnston, *J. Phys. Chem.*, 1978, **82(3)**, 254-268.
- 224 (14) J. A. Robinson, M. A. Bergougnou, W. L. Cairns, G. S. P. Castle and I. I. Inculet, *IEEE*
225 *Trans. Ind. Appl.*, 1998, **34(6)**, 1218-1224.

- 226 (15) K. Takaki, I. Yagi, T. Fujiwara and T. Go, *IEEE Trans. Dielectr. Electr. Insul.*, 2011,
227 **18(5)**, 1752-1758.

228 Table 1. Inlet gas concentration

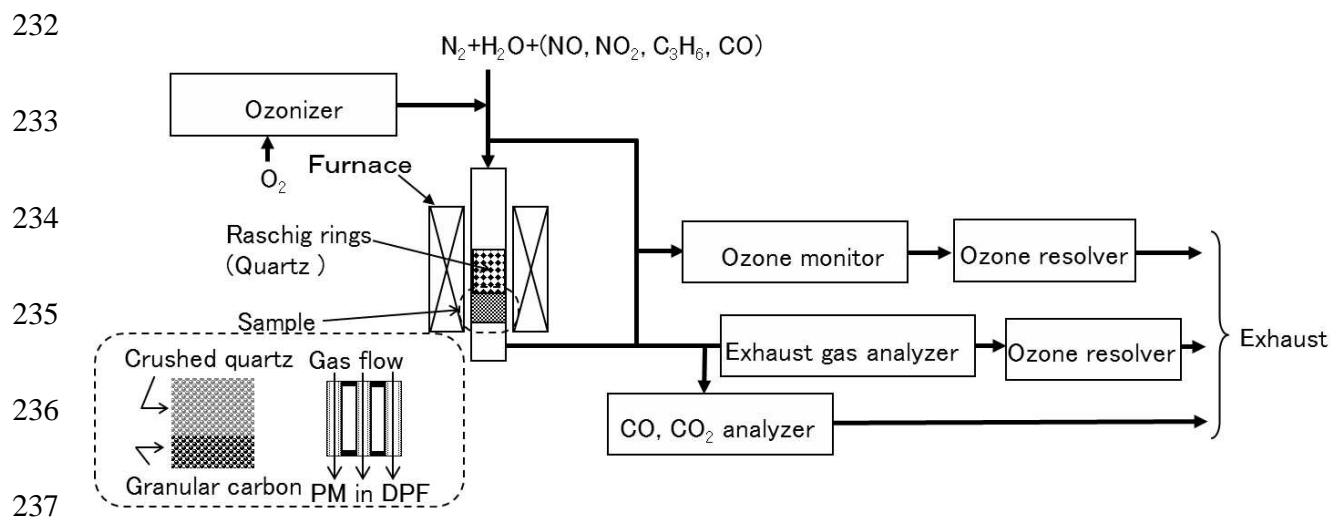
	Concentration							
	O ₃	NO	NO ₂	C ₃ H ₆	CO	O ₂	H ₂ O	N ₂
	(ppm)	(ppm)	(ppm)	(ppm C)	(ppm)	(%)	(%)	
PM and C ox.	0-930	0-550	0-550	-	-	10	3	balance
O ₃ decomp.	0-930	-	-	-	-	10	3	balance
O ₃ react	400-930	0-550	0-550	0-1000	0-1000	10	3	balance

229

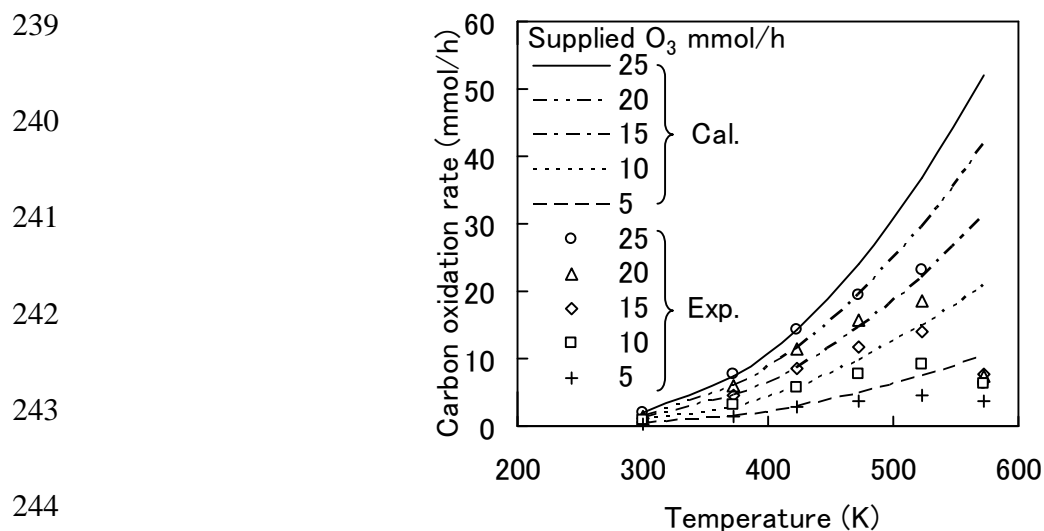
230 Table 2. Inlet gas temperature and total gas flow rate

	Inlet gas temperature	Total gas flow rate
	(K)	(L/min)
PM and C ox.	298-573 (steady-state)	10
O ₃ decomp.	298-573 (heating 10 K/min)	10
O ₃ react.	298-573 (steady-state)	10

231



238 Figure 1. Experimental set-up



245 Figure 2. Experimental and calculated (without thermal decomposition of ozone) temperature
246 dependence of carbon oxidation rate; 190-930 ppm ozone, 300-573 K.

247

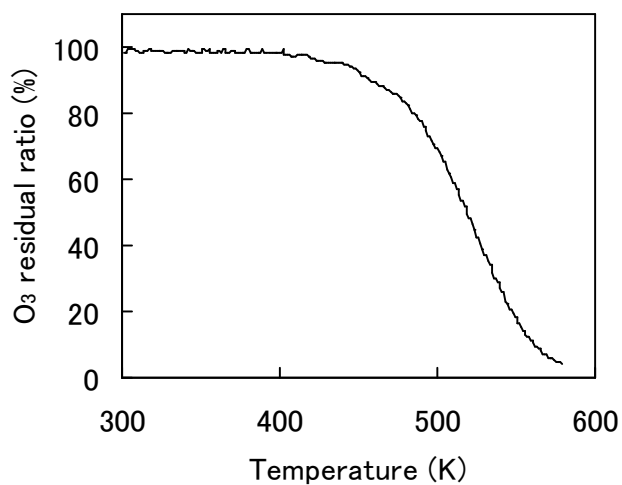
248

249

250

251

252



253 Figure 3. Temperature dependence of ozone residual ratio; 550 ppm ozone, 300-573 K.

254

255

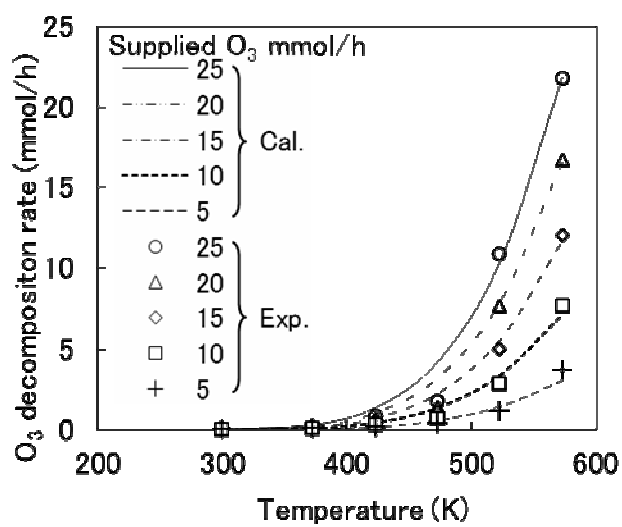
256

257

258

259

260



261 Figure 4. Experimental and calculated temperature dependence of the ozone decomposition rate;

262 190-930 ppm ozone, 300-573 K.

263

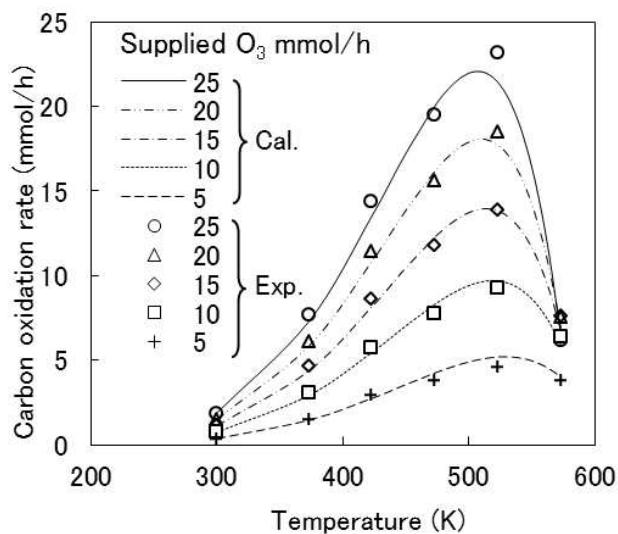
264

265

266

267

268



269 Figure. 5. Experimental and calculated (with thermal decomposition of ozone) temperature
 270 dependence of the carbon oxidation rate using ozone; 190-930 ppm ozone, 300-573 K.

271

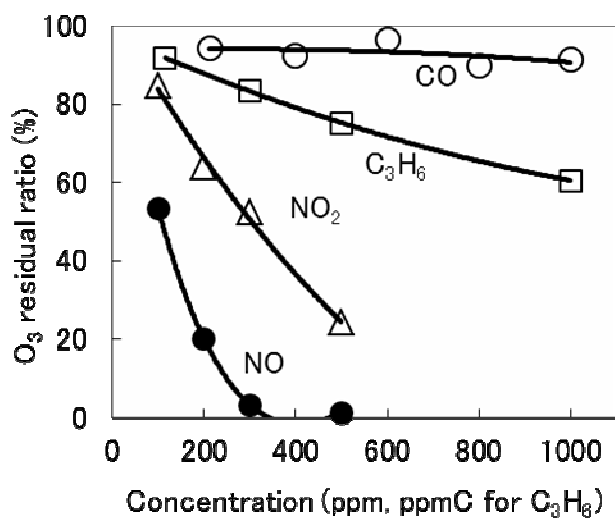
272

273

274

275

276



277 Figure 6. Ozone residual ratio containing other gas components; 400 ppm ozone, 423 K

278

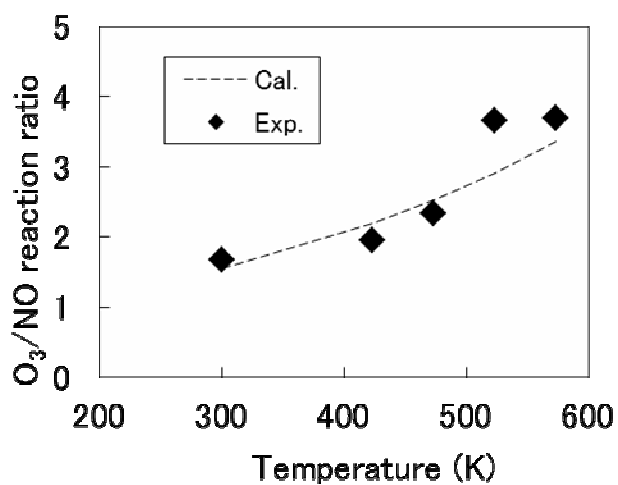
279

280

281

282

283



284 Figure 7. Calculated and experimental temperature dependence of ozone/NO reaction ratio; 550-
285 930 ppm ozone, 100-500 ppm NO.

286

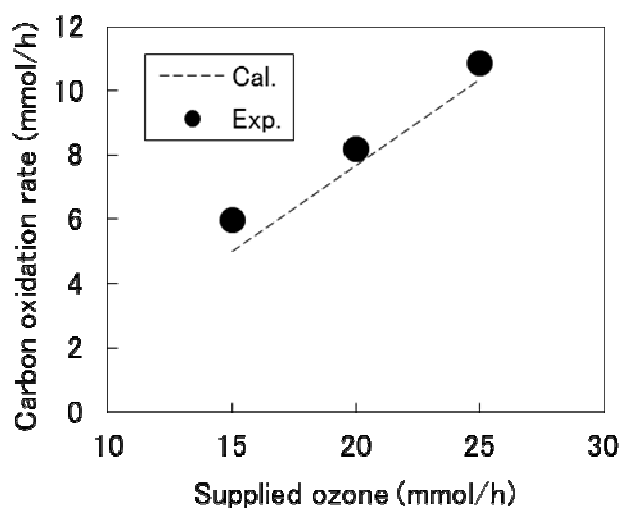
287

288

289

290

291



292 Figure 8. Experimental and calculated carbon oxidation rate using ozone containing NO and
293 allowing for the thermal decomposition of ozone; 560-930 ppm ozone, 100 ppm NO, at 423 K.

294

295

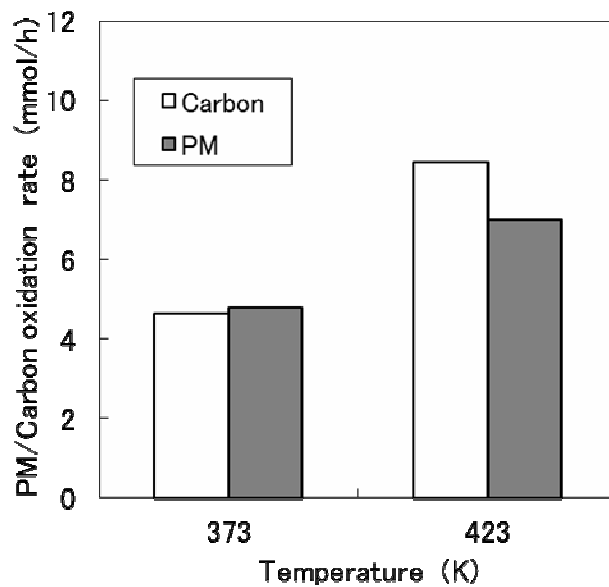
296

297

298

299

300



301 Figure 9. Comparison of oxidation rate for carbon and PM using ozone; 550 ppm ozone, at 373
302 and 423 K.

303

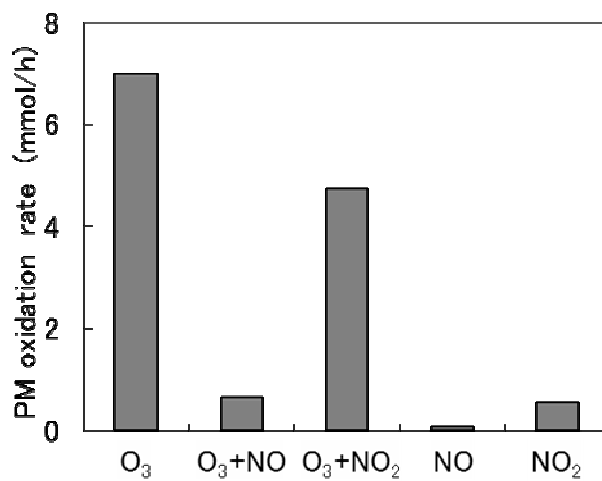
304

305

306

307

308



309 Figure 10. Comparison of PM oxidation rates using ozone, NO, and NO₂, and mixtures thereof;
310 550 ppm ozone, NO and NO₂, 423 K.